# Complexation of $Li^+$ and $Cu^+$ with HX (X = F, Cl, OH, SH, $NH_2$, and $PH_2$) Molecules by B3LYP and CCSD(T) Methods

**Ahmed M. El-Nahas*,† and Kimihiko Hirao**

*Department of Applied Chemistry, Graduate School of Engineering, The University of Tokyo, Hongo, Tokyo 113-8656, Japan*

*Received: August 18, 1999; In Final Form: October 27, 1999*

B3LYP and CCSD(T) calculations have been performed to determine binding energies (BE) and electronic structures of $Li^+$ and $Cu^+$ in their interaction with small ligands of the type HX (X = F, Cl, OH, SH, $NH_2$, and $PH_2$). BE of all ligands with $Cu^+$ are higher than with $Li^+$ with the exception of FH. For almost all ligands, the second ligand binds stronger than the first with $Cu^+$ whereas the opposite trend was found for $Li^+$ species. Water and ammonia bind with $Cu^+$ by approximately the same bond length but the BE is 14 kcal/mol higher for $NH_3$ because the latter is superior with respect to polarizability, induced dipole moments, charge transfer (CT), and $sd_\sigma$ effects. Different from other ligands studied here, $PH_3$ complexes are dominated by CT from the hydrogen atoms to the metal center through the phosphorus atom, leading to a different behavior of the ligand geometry changes when forming a complex. The MP*n* and CCSD(T) with TZP plus diffuse functions are necessary for accurate estimation of binding energies for $Cu^+$ complex.

## Introduction

Molecules containing transition metal ions are of considerable interest because of their many catalytic and materials applications. Experimental investigations were concerned with $Li^+$ and $Cu^+$ complexes bound with water and ammonia ligands.[1−10] These studies indicated that $Cu^+$ binds with the second water and/or ammonia ligands as strong as the first ones. The third and fourth ligands are much less bound compared to the first two. This is the general trend in most of the transition metal ion complexes with small ligands.[1−8] On the other hand, the successive binding energies in water−alkali metal ion complexes decrease slowly with increasing number of ligands.[9,10] Many theoretical works have dealt with binding energies for alkali and transition metal ion complexes.[11−35] Various mechanisms were proposed for explaining the great variation in the successive binding energies. These include electrostatic, dative, covalent, and the way available to the metal atom to reduce repulsion with the incoming ligand, such as s−p polarization, and s−$d_\sigma$ hybridization. Recently, we have analyzed these phenomena in detail for $Cu^+(XH)_n$, X = OH, $NH_2$, $n = 1−4$.[22]

With the exception of few studies[18−21] including $H_2S$ and $PH_3$, most of the theoretical studies have concentrated on transition metal ion complexes with water and ammonia molecules. Sulfur- and phosphorus-containing ligands are of fundamental importance in chemistry. The FH, ClH, $H_2S$, and $PH_3$ ligands have been used with alkali metal ions in previous theoretical studies.[11−17] Therefore, we selected $Cu^+$ from transition metals and $Li^+$ from alkali metals to examine their interactions with XH, X = F, Cl, OH, SH, $NH_2$, and $PH_2$, for one and two ligands. To the best of our knowledge, this is the first study containing direct comparison between $Li^+$ and $Cu^+$ using this set of ligands. $Li^+$ is the closet alkali metal ion to $Cu^+$ with respect to their ionic radii and we expect some similarities between them. In the present work we have three objectives:

The first one concerns determining the binding energies and electronic structures of $Li^+/Cu^+(XH)_n$ (X = F, Cl, OH, SH, $NH_2$, and $PH_2$), $n$ = 1,2, across the row and down the column in the periodic table. The second one is the highlighting of the difference between the behavior of $Li^+$ and $Cu^+$ when bind to these ligands. Finally, we would like to address the computational requirements for obtaining accurate binding energies in monopositive alkali and transition metal ion complexes with a variety of small neutral ligands.

## Calculations

All geometries have been fully optimized without symmetry constraints using the B3LYP DFT[36] method. The 6-311+G(d,p) basis set[37] was employed for all atoms except Cu. For Cu, the Ne core was replaced by the effective potential of Hay and Wadt[38] while the valence orbitals were treated by Gaussian basis functions of double-ζ quality which is a [3s3p2d] contraction of a (5s5p5d) primitive set.[37] For the sake of simplicity, we will refer to the above-mentioned basis sets as basis 1. In our previous work,[22] the basis set superposition error (BSSE) in $Cu^+OH_2$ using cc-pVDZ for $H_2O$ and LANL2DZ for copper was 5.4 kcal/mol, 0.5 of which comes from the lowering of the Cu energy by $H_2O$ basis set. This BSSE is greatly reduced when the basis set is extended to triple-ζ quality.[22,24] It has been reported that the addition of the second polarization function has little effect on the binding energies.[33] The diffuse functions used were found to be important when interactions with systems containing lone pair of electrons are studied.[33] Frequency calculations at B3LYP/basis 1 were performed for optimized species in order to determine the nature of stationary points as minima or transition states and to obtain zero-point energy (ZPE) corrections.

Accurate binding energies of $Cu^+$ demand high computational levels, both in term of one-electron basis set and treatment of

---

[†] Permanent address: Chemistry Department, Faculty of Science, El-Menoufia University, Shebin El-Kom, Egypt.

10.1021/jp9929115 CCC: $19.00

electron correlation.[18,19,22−28,34,35] In the case of alkali-metal ion complexes moderate levels of calculations reproduce the experimental binding energies as the interaction is mainly electrostatic.[11−17] For final energy calculations, the same basis sets were used with the coupled cluster method including single, double, and a perturbative treatment of triple excitations (CCSD(T)).[37] For some selected systems we have calculated binding energies using different basis sets to investigate basis set effects.[37]

The induced dipole moments on the metal ions and ligands are calculated at B3LYP/basis 1 according to

$$\Delta\mu(M^+) = 2\alpha(M^+)\Delta\mu(L)/R^3 \tag{1}$$

$$\Delta\mu(L) = q(M^+)\alpha(L)/R^2 \tag{2}$$

where $q$, $\mu$, and $\alpha$ are respectively the static charge, dipole moment, and polarizability of the fragment and $R$ the M−L bond length.

The hardness ($\eta$) of a chemical species was calculated at B3LYP/basis 1 from

$$\eta = (I - A)/2$$

with $I$ and $A$ representing the ionization potential and electron affinity, respectively.

Energy partitions were computed by Morokuma analysis[39] implemented in the Gamess program.[40] NBO analysis was also performed to analyze orbital occupation and the contribution of atomic orbitals in a given molecular orbital as well as calculating the natural charges.[41] All calculations were performed with the Gaussian 98 suite of programs.[37]

## Results and Discussion

**Structures**. The optimized geometries for the systems under investigation are displayed in Figure 1. The corresponding geometrical parameters are listed in Table 1. In the case of $NH_3$ and $PH_3$, there is only one lone pair of electrons which aligns in the direction of the molecular dipole and, therefore, one structure will be formed where the cation is directed toward the dipole of the ligand. One of the two lone pairs of $H_2O$ and $H_2S$ coincides with the direction of the molecular dipole; the second one is perpendicular to the molecular plane. Therefore, two orientations are possible for binding to a cation. The first structure is planar with $C_{2v}$ symmetry where the cation is aligned with the direction of the dipole moment as in the case of $H_2O$. The second one is preferred when covalent contribution to bonding is high and this produces pyramidal structure of $C_s$ symmetry as in the case of $H_2S$ with both ions. The loss of ion−dipole interaction in the pyramidal $M^+-SH_2$ systems is compensated by charge transfer. $H_2S$ interacts with $Cu^+$ through the high 3p orbital leading to a structure in which the Cu−S axis is nearly perpendicular (99.1°) to the HSH plane, with a HSH angle of 93.9°. The planar forms are 10.3 and 5.6 kcal/mol less stable in the case of $Cu^+$ and $Li^+$, respectively, at CCSD(T)/basis 1//B3LYP/basis 1. Planarization of $H_2S$ demands energy for s−p hybridization, which reduces the stability of the planar system. Previous studies indicated the higher stability of the pyramidal forms of $Cu^+SH_2$ and $Li^+SH_2$ complexes over the planar ones.[17,18] A difference of 8.1 kcal/mol has been found for $Cu^+SH_2$ species at MP2/DZP level.[18]

In complexation with the FH molecule, $Li^+$ binds in the direction of the dipole leading to linear structure (LiFH angle is 180.0°) while Cu $^+$ binds in the direction of one of the lone pairs leading to a bent structure (CuFH angle is 148.0°). The bending energies are small in both systems and were estimated to be 0.3 kcal/mol. The same phenomena happened for the interaction of $H_2CO$ with $Cu^+$ and $Na^+$.[18] Both $Li^+$ and Cu $^+$ bind to one of the lone pairs of ClH molecule leading to bent structures (HClM angles are 106.0° and 102.3°, respectively).

From the percent contribution of each fragment in the Cu−L bonding, it is clear that the covalency increases with the softness of the ligand with $PH_3$ standing as the most covalent one (Table 2). The Cu−L bond distances increase with increasing $Z$ of the central atom of the ligand in the same row in the periodic table. This shortening of the bond length occurs because the polarization in $Cu^+$ (3.33 au for $Cu^+$ at B3LYP/basis 1) pushes the electron density away from the ligand direction. In addition, $4s-3d_\sigma$ hybridization increases in going from FH to $NH_3$. The polarization of the $Cu^+$ ion performs the same role as $sd_\sigma$ hybridization does; see Table 2 for the percent of 4s and 3d contribution to the HOMO in $Cu^+$ complexes and Table 6 for the polarization contribution in $Cu^+$ compared to a zero contribution for $Li^+$. In addition, charge transfer leads to shorter bonds. On the contrary, the Li−L bond lengths increase across the row due to the absence of polarization, sp or $sd_\sigma$ hybridization, and charge transfer. The only variable is the increase of the ligand size which gives rise to longer Li−L bonds.

The two-ligand systems are linear with a bending potential ranging from 0.2 to 4.8 kcal/mol for $Cu^+$ complexes which indicates the attenuation of $sd_\sigma$ hybridization upon bending. On the other hand, the corresponding values for $Li^+$ adducts range from 0.1 to 0.8 kcal/mol, which shows $Li^+$ systems as quasilinear. Earlier studies on $Cu^+$ and $Li^+$ complexes predicted the linear structure as the only stable form of $M^+(L)_2$.[12,13,15,22,24,35] All attempts to find a lower symmetry conformation resulted in slow collapse back to the linear one.

In going from the mono- to diligated systems, the Cu−L bond lengths decreased for all but $H_2S$ and $PH_3$ where they are unchanged for the former and increased for the latter. This can be attributed to the effect of the first ligand as can be seen from 4s population listed in Table 2. Transferring more electrons from the first ligand resists more charge transfer (CT) from the second one which in turn affect the Cu−L bond distance. The shortening of the M−L bond lengths upon the addition of the second ligand has been noticed for complexes containing transition metal ions, while alkali metal ions with different ligands give longer M−L bond distances for the second ligand. [12,13,15,22,24,35]

There are three unpaired electrons in the valence shells of the N and P atoms. These unpaired electrons are in p orbitals, so that, without hybridization, valence angles are expected to be around 90°. The experimental and computed valence angles of free $PH_3$ show that the bonds use almost pure p orbitals with little or no hybridization. In $NH_3$, however, the valence angle is only a little less than the tetrahedral angle, which means that the N atom is hybridized almost tetrahedrally. Table 1 shows that the valence angle in $NH_3$ is little affected by forming a complex. However, the valence angle in $PH_3$ is significantly widened from 93.5° to 102.6° upon complexation. We have optimized $PH_3$ and $Cu^+PH_3$ at the MP2/basis 1 level and obtained the same results. This anomaly of $PH_3$ comes from two reasons. One is the use of s and p orbitals and the other is purely electrostatic.

For the free $PH_3$, the PH bonds are not polarized since there is a little electronegativity difference between P and H atoms. Thus, the P−H bond is covalent in character. Upon forming a complex with $Cu^+$, CT occurs from the three hydrogen atoms to $Cu^+$ through P, leading to a resultant net positive charge around each hydrogen and a slightly net negative charge around

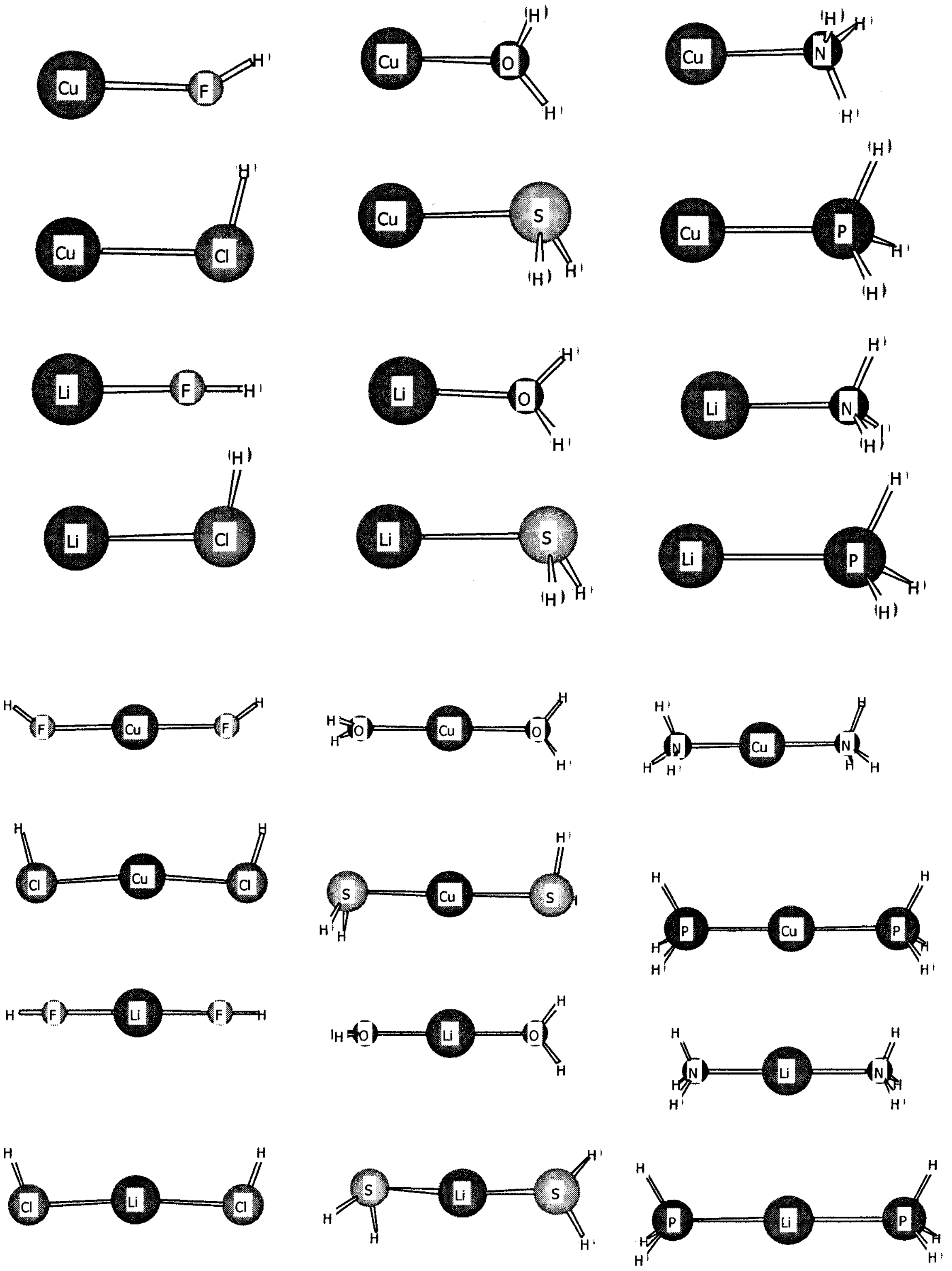

**Figure 1.** Optimized structures for $Li^+$/$Cu^+$ complexes at B3LYP/basis 1.

P. Thus, each P−H bond involves covalent-ionic resonance. The positive charges around hydrogen atoms will repel each other with a Coulombic force, and so the HPH angle is increased compared to that of free ligand. This geometrical change enhances the $sp^3$ hybridization of the P atom. It is deduced from the percent contribution of the s and p orbitals of P in Table 2. As the percent of the s character increases the P−H bond lengths become shorter and HPH angles are widened. The same phenomena happened with $Li^+PH_3$ but the effect is smaller than with $Cu^+PH_3$. The cost of the hybridization for $PH_3$ in $Cu^+$-$PH_3$ amounted to ∼23 kcal/mol at the CCSD(T)/basis 1//B3LYP/basis 1 by calculating the energy of the free $PH_3$ and that in the complex ignoring the cation. The geometries of FH, $OH_2$, ClH, and $SH_2$ are hardly affected by complexation. For these ligands, charges are transferred from both heavy and hydrogen atoms as detected from charge variation in the ligand upon complex formation.

**Binding Energies**. In Tables 3−5, ZPE corrected binding energies (BE) at different levels are collected. The B3LYP and CCSD(T) values are plotted against type and number of ligands

**TABLE 1: Geometrical Parameters for $Li^+$ and $Cu^+$ Complexes and Induced Dipole Moment on Ligands, and Hardness, Polarizability, and Geometries of Different Ligands at B3LYP/Basis 1**[a]

| species | M−X | X−H | ∠MXH | ∠HXH | ∠XMX | $\mu_{ind}$ | species | $\eta$ | α | H−X | ∠HXH |
|---|---|---|---|---|---|---|---|---|---|---|---|
| $Cu^+-FH$ | 2.052 | 0.936 | 148.3 | | | 0.49 | FH | 9.4 | 3.9 | 0.922(0.917) | |
| $Cu^+-OH_2$ | 1.965 | 0.966 | 125.9 | 108.2 | | 1.13 | $OH_2$ | 7.8 | 8.3 | 0.962(0.957) | 105.0(104.5) |
| $Cu^+-NH_3$ | 1.961 | 1.021 | 112.0 | 106.8 | | 1.87 | $NH_3$ | 6.4 | 13.6 | 1.014(1.012) | 107.9(106.7) |
| $Cu-^+ClH$ | 2.317 | 1.300 | 102.3 | | | 1.33 | ClH | 7.2 | 13.5 | 1.287 (1.275) | |
| $Cu^+-SH_2$ | 2.281 | 1.355 | 99.1 | 93.9 | | 2.43 | $SH_2$ | 5.9 | 23.9 | 1.348 (1.336) | 92.5(92.1) |
| $Cu^+-PH_3$ | 2.257 | 1.406 | 115.7 | 102.6 | | 3.43 | $PH_3$ | 5.8 | 33.3 | 1.423(1.411) | 93.5(93.3) |
| $Cu^+-PH_3$ | (2.294 | 1.395 | 116.3 | 101.9)[b] | | | $PH_3$ | | | 1.409[b](1.411) | 94.3[b](93.3) |
| $HF-Cu^+-FH$ | 2.026 | 0.934 | 142.6 | | 170.4 | | $Cu^+$ | 6.5 | 3.3 | | |
| $H_2O-Cu^+-OH_2$ | 1.939 | 0.965 | 125.7 | 108.5 | 180.0 | | $Li^+$ | 35.2[c] | 0.2 | | |
| $H_3N-Cu^+-NH_3$ | 1.950 | 1.020 | 112.3 | 106.5 | 180.0 | | | | | | |
| $HCl-Cu^+-ClH$ | 2.304 | 1.299 | 102.5 | | 172.3 | | | | | | |
| $H_2S-Cu^+-SH_2$ | 2.288 | 1.354 | 100.2 | 93.8 | 175.9 | | | | | | |
| $H_3P-Cu^+-PH_3$ | 2.293 | 1.408 | 117.1 | 100.9 | 180.0 | | | | | | |
| $Li^+-FH$ | 1.801 | 0.934 | 179.7 | | | 0.64 | | | | | |
| $Li^+-OH_2$ | 1.841 | 0.967 | 127.1 | 105.8 | | 1.29 | | | | | |
| $Li^+-N\ H_3$ | 1.970 | 1.021 | 113.6 | 105.1 | | 1.85 | | | | | |
| $Li^+-ClH$ | 2.328 | 1.297 | 106.0 | | | 1.32 | | | | | |
| $Li^+-SH_2$ | 2.413 | 1.352 | 102.3 | 94.1 | | 2.17 | | | | | |
| $Li^+-PH_3$ | 2.492 | 1.410 | 118.3 | 99.4 | | 2.84 | | | | | |
| $HF-Li^+-FH$ | 1.821 | 0.932 | 178.9 | | 179.6 | | | | | | |
| $H_2O-Li^+-OH_2$ | 1.868 | 0.966 | 127.0 | 105.8 | 179.3 | | | | | | |
| $H_3N-Li^+-NH_3$ | 2.000 | 1.020 | 113.4 | 105.2 | 180.0 | | | | | | |
| $HCl-Li^+-ClH$ | 2.349 | 1.296 | 106.4 | | 173.9 | | | | | | |
| $H_2S-Li^+-SH_2$ | 2.437 | 1.351 | 102.8 | 94.4 | 176.8 | | | | | | |
| $H_3P-Li^+-PH_3$ | 2.521 | 1.411 | 118.8 | 98.7 | 180.0 | | | | | | |

[a] Bond lengths in Å, bond angles in deg, $\mu_{ind}$ in debyes, $\eta$ in eV, and α in au. [b] MP2/basis 1 values. [c] Experiment 35.22 eV.

**TABLE 2: Relative Contributions of the $Cu^+$ and X Hybrids to the Cu−X Bond, Populations 4s of $Cu^+$ and 2s of $Li^+$, Percent of 4s−3d Mixing in the HOMO Orbitals of $Cu^+$ Species, and Natural Charges on $Cu^+$ and $Li^+$ at B3LYP/Basis 1**

| | $Cu^+FH$ | $Cu^+OH_2$ | $Cu^+NH_3$ | $Cu^+ClH$ | $Cu^+SH_2$ | $Cu^+PH_3$ |
|---|---|---|---|---|---|---|
| total % Cu | | | **6.7** | **5.2** | **10.4** | **14.4** |
| % 4s | | | 95.3 | 94.5 | 95.8 | 96.4 |
| % 3d | | | 3.6 | 1.7 | 1.9 | 1.9 |
| % 4P | | | 1.1 | 3.8 | 2.4 | 1.7 |
| total % X | | | **93.3** | **94.8** | **89.6** | **85.6** |
| % ns | | | 20.1 | 7.4 | 7.9 | 24.3 |
| % np | | | 79.9 | 92.4 | 91.9 | 75.5 |
| % 4s, % 3d | 0.7, 99.3 | 2.2, 97.8 | 3.5, 96.4 | 1.1, 98.9 | 1.4, 98.6 | 2.0, 98.0 |
| populn of 4s | 0.03 | 0.08 | 0.2 | 0.12 | 0.24 | 0.32 |
| populn of 2s | 0.0 | 0.0 | 0.02 | 0.02 | 0.03 | 0.04 |
| $Q_{Cu^+}$ | 0.990 | 0.966 | 0.878 | 0.900 | 0.805 | 0.745 |
| $Q_{Li^+}$ | 0.995 | 0.990 | 0.979 | 0.969 | 0.953 | 0.942 |

| | $Cu^+(FH)_2$ | $Cu^+(OH_2)_2$ | $Cu^+(NH_3)_2$ | $Cu^+(ClH)_2$ | $Cu^+(SH_2)_2$ | $Cu^+(PH_3)_2$ |
|---|---|---|---|---|---|---|
| total % Cu | | | **8.7** | **7.0** | **11.8** | **15.0** |
| % 4s | | | 90.6 | 94.6 | 94.3 | 95.2 |
| % 3d | | | 9.4 | 4.2 | 4.8 | 4.3 |
| % 4P | | | 0 | 1.2 | 0.9 | 0.5 |
| total % X | | | **91.3** | **93.0** | **88.2** | **85.0** |
| %ns | | | 25.4 | 13.1 | 13.4 | 30.1 |
| % np | | | 74.6 | 86.8 | 86.4 | 69.8 |
| % 4s, % 3d | 3.8, 96.2 | 7.7, 92.3 | 9.7, 90.3 | 3.7, 96.4 | 4.9, 95.1 | 4.3, 95.7 |
| populn of 4s | 0.13 | 0.29 | 0.48 | 0.32 | 0.49 | 0.58 |
| populn of 2s | 0.01 | 0.03 | 0.08 | 0.07 | 0.11 | 0.16 |
| $Q_{Cu^+}$ | 0.950 | 0.864 | 0.706 | 0.743 | 0.601 | 0.532 |
| $Q_{Li^+}$ | 0.982 | 0.961 | 0.916 | 0.911 | 0.861 | 0.822 |

in Figure 2. Only a few experimental data are available for comparison and these are also included in Tables 3−5. The second ligand for $Cu^+$ binds comparable to the first or even higher whereas for $Li^+$ the second is usually lower. An inspection of Table 3 and Figure 2 indicates that the calculated BE for $Li^+$ adducts at B3LYP and CCSD(T) are comparable. The corresponding values for $Cu^+$ complexes differ by up to ~10 kcal/mol (Tables 4 and 5). Obviously, B3LYP overestimates the binding of $Cu^+$ complexes compared to CCSD(T). CCSD(T) reproduces the experimental tendency of BE(1st) < BE(2nd) for $Cu^+$ complexes while B3LYP yields the reverse trend. Previously, we have reported the overestimation of the binding energies of $Cu^+$ complexes by B3LYP, BLYP, and BP86 functionals.[22] Probably we can say that DFT methods overestimate the binding energy of the first ligand and, consequently, reverse the order for the first two ligands. On the other hand, ab initio calculations at post-HF levels give the correct order due to the improvement of the $sd_\sigma$ hybridization. The BEs of $Li^+$-containing complexes are insensitive to theoretical levels as reported before,[11−17] whereas for $Cu^+$ systems sophisticated levels are needed, both in terms of one-electron basis set and treatment of electron correla-

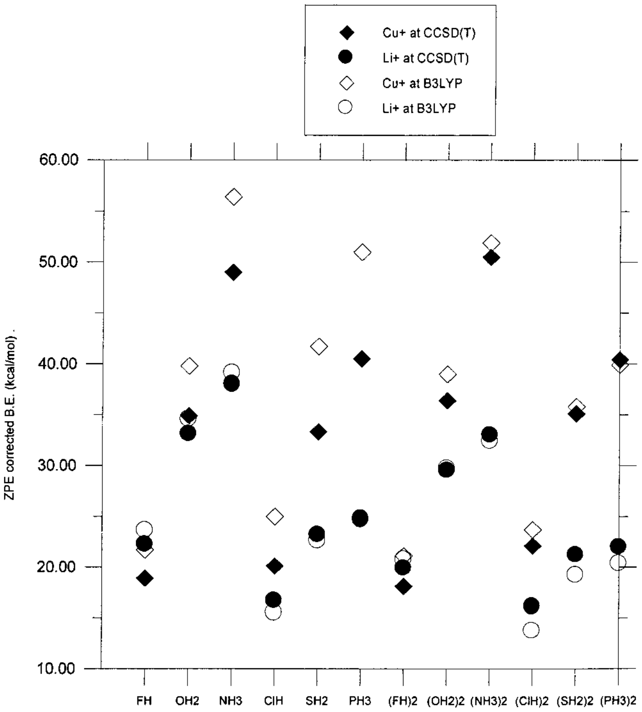

**Figure 2.** BEs. for $Li^+/Cu^+$ complexes at CCSD(T)/basis 1 and B3LYP/basis 1 against type and number of ligands.

tion.[18,19,22−28,34,35] Our calculated binding energies agree with the available experimental data for $Cu^+$ and $Li^+$ complexes as well as with theoretical results from other studies.[2,6,10,18,19,22−28,34,35]

Increased softness of the ligand raises the demand for higher correlation. In the case of FH, the hardest ligand studied here, the BE is slightly affected by using high correlation but for other ligand, especially for second-row ligands, the gap between B3LYP and MP*n* and CCSD(T) values increases. For instance, hydrogen sulfide is significantly affected by correlation than water. Moreover, the BE of first ligand is strongly affected by electron correlation than the second one. Table 5 indicates the importance of TZ quality basis sets and diffuse functions for accurate calculation of BE, but no improvement is achievedby using the second polarization functions. However, all theoretical results agree within the uncertainty of the experimental data, except for $Cu^+(NH_3)_{1,2}$ where there is a great uncertainty in the experimental results.[6] Theory supports a $Cu^+NH_3$ binding energy of 49 kcal/mol. Bauschlicher et al.[24] have calculated a value of 52 kcal/mol for BE of $Cu^+NH_3$ complex at MCPF/TP2P level.

From Tables 3 and 4, the following BE orders are assigned for $Li^+$ at CCSD(T): $NH_3 > H_2O > PH_3 > H_2S > FH > ClH$, whereas for $Cu^+$ at CCSD(T) $NH_3 > PH_3 > H_2O > H_2S > ClH > FH$. The B3LYP orders agree in all systems, except for FH and $H_2S$ for $Li^+$ and $H_2O$ and $H_2S$ for $Cu^+$, where the binding energies are somewhat comparable.

Within the same row, the binding energy order parallels the softness of the ligands where $NH_3 > H_2O > FH$ and $PH_3 > H_2S > ClH$. From Tables 2 and 4, on comparing first- and second-row ligands in their binding to $Cu^+$, we found that the binding energies are directly proportional to the percent of $sd_\sigma$ but within the same row, it is directly proportional to 4s population, $\%sd_\sigma$, and inversely proportional to bond lengths and charge on Cu. Generally, systems with higher $\%sd_\sigma$ have higher binding energies.

On comparing $Cu^+$ with $Li^+$, we have to remember that charges transfer easily to $Cu^+$ than $Li^+$ as the former has a higher ionization potential (7.7 vs 5.4 eV).[42] The polarizability of $Cu^+$ is 3.33 au at B3LYP/LANL2DZ, which means that the neighboring ligand can induce a sizable dipole moment at $Cu^+$. On the other hand, $Li^+$ has a very small polarizabilty (0.2 au at B3LYP/basis 1), so that $Li^+$ has effectively no induced dipole moment. Second-row ligands bind at longer distances than their first-row counterparts and, therefore, generalization is difficult because the electrostatic interaction is attenuated at long separation.

For $Li^+$ adducts, the first-row ligands bind to $Li^+$ stronger than their second-row analogues by 6−13 kcal/mol. This can be attributed to the electrostatic contribution to the binding energies which are higher in the case of the first-row molecules; compare 23.3, 40.7, and 48.9 kcal/mol with 11.2 19.4, and 23.7 kcal/mol for XH, X = F, OH, $NH_2$, Cl, SH, $PH_2$, respectively (Table 6). On moving across the first-row ligands ($FH \rightarrow NH_3$), electrostatic, polarization, and charge transfer contributions to the total interaction energies increase, which explains the gradually increased BE.

Increasing softness of the ligand favorsbinding to $Cu^+$ more than to $Li^+$. The $Cu^+$ is a soft acid while $Li^+$ is a hard one; the corresponding hardness values are 6.5 and 35.2 eV (Table 1). On the basis of the hard−soft acid−base (HSAB) principle,[43] hard acid binds strongly to hard base and soft acid bind weakly to hard base. On comparing between $Li^+$ and $Cu^+$ in their binding to FH and ClH, we found that FH binds strongly to $Li^+$ than to $Cu^+$ whereas ClH binds strongly to $Cu^+$ compared to $Li^+$. This is because FH is a harder base than ClH by ∼2 eV. The interaction of $H_2O$ and $H_2S$ with cations was investigated for many cationic moieties either metallic or organic.[11−19,44,45] Both compete in their effects depending on the level of theory. But it has been mentioned that description of the interaction involving $H_2S$ needs higher correlated levels to account for the electronic effects of $H_2S$.[18] Despite higher CT involved for $PH_3$ in its interaction with $Cu^+$, $NH_3$ still has higher BE due to higher electrostatic interaction in the latter case (Tables 6 and 7). Moreover, geometrical changes occurringin $PH_3$-containing systems cost energy as mentioned earlier.

## Morokuma Analysis

The results of Morokuma analysis are presented in Tables 6 and 7. The order of electrostatic component in both $Li^+$ and $Cu^+$ systems parallels the total binding energies. This indicates the predominance of the electrostatic mechanism. The polarization term contributes 1−9 kcal/mol to the binding energies for $Cu^+$ while for the ligands it contributes 8−35 kcal/mol. In addition, a sizable charge transfer to $Cu^+$ contributes to the BEs. The CT increases with increasing base softness. This is reflected in 4s population (Table 2), and from CT energy contribution to the interaction energy (Table 6).

Generally speaking, electrostatic interactions favor $Li^+$ over $Cu^+$ whereas polarization and charge-transfer effects favor $Cu^+$ (see Table 7). It is also clear that the electrostatic term is the main factor behind the higher BE of $Li^+FH$ compared to $Cu^+$-FH. For $Li^+$, the electrostatic term is higher than the polarization one in the case of first-row ligands but for the second-row analogues the polarization is higher. On the other hand, for $Cu^+$ the polarization is higher for all ligands. $NH_3$ is more bound to $Cu^+$ than $PH_3$ by about 8.5 kcal/mol. In an attempt to rationalize this difference, we have compared corresponding terms in the Morokuma analysis. CT is more stabilizing for $PH_3$ by 6.2 kcal/mol, and PL is more stabilizing for $NH_3$ by 0.9 kcal/mol. ES is

**TABLE 3: ZPE-Corrected First and Second Ligand BE (kcal/mol) for $Li^+(XH)_{1,2}$ Systems at B3LYP/Basis 1 and CCSD(T)/Basis 1//B3LYP/Basis1**

| M/L | FH | $OH_2$ | $NH_3$ | ClH | $SH_2$ | $PH_3$ | $(FH)_2$ | $(OH_2)_2$ | $(NH_3)_2$ | $(ClH)_2$ | $(SH_2)_2$ | $(PH_3)_2$ |
|---|---|---|---|---|---|---|---|---|---|---|---|---|
| B3LYP | 23.6 | 34.6 | 39.1 | 15.5 | 22.6 | 24.7 | 20.7 | 29.7 | 32.4 | 13.7 | 19.2 | 20.3 |
| CCSD(T) | 22.2 | 33.1 | 38.0 | 16.7 | 23.2 | 24.8 | 19.9 | 29.5 | 33.0 | 16.1 | 21.2 | 22.0 |
| expt | | 34.0[a] | 39.1[b] | | | | | | | | | |

[a] Reference 9. [b] Reference 10.

**TABLE 4: ZPE-Corrected First and Second Ligand BE (kcal/mol) for $Cu^+$ Complexes at Level/Basis 1//B3LYP/Basis 1**

| level/L | FH | $OH_2$ | $NH_3$ | ClH | $SH_2$ | $PH_3$ | $(FH)_2$ | $(OH_2)_2$ | $(NH_3)_2$ | $(ClH)_2$ | $(SH_2)_2$ | $(PH_3)_2$ |
|---|---|---|---|---|---|---|---|---|---|---|---|---|
| B3LYP | 21.7 | 39.8 | 56.4 | 25.0 | 41.7 | 51.0 | 21.1 | 39.0 | 51.9 | 23.7 | 35.8 | 39.9 |
| MP2 | 19.1 | 35.7 | 50.6 | 20.5 | 34.2 | 42.8 | 18.1 | 37.4 | 52.4 | 22.4 | 36.3 | 42.6 |
| MP4SDQ | 19.6 | 36.5 | 51.5 | 21.0 | 35.0 | 43.8 | 18.9 | 39.3 | 54.6 | 23.5 | 38.0 | 44.9 |
| CCSD | 18.9 | 34.7 | 48.3 | 19.4 | 32.1 | 39.1 | 18.0 | 35.6 | 49.0 | 21.1 | 33.6 | 38.7 |
| CCSD(T) | 18.9 | 34.9 | 49.0 | 20.1 | 33.3 | 40.5 | 18.1 | 36.4 | 50.5 | 22.1 | 35.1 | 40.4 |
| expt | | 35 ± 3[a] | 49[c] | | | | | 39 ± 3[a] | 59 ± 2.4[b] | | | |
| expt | | | 56 ± 3.6[b] | | | | | | | | | |

[a] Reference 2. [b] Reference 3. [c] Reference 6.

**TABLE 5: First and Second Ligand BE at Different Levels for $Cu^+(XH_2)_n$ ($X = O, S$; $n = 1, 2$) Systems (LANL2DZ Basis Set Is for Cu)**

| level of computation/experiment | BE(1st) X = O | BE(2nd) X = O | BE(1st) X = S | BE(2nd) X = S |
|---|---|---|---|---|
| B3LYP/cc-pvDZ//B3LYP/cc-pVDZ | 47.8 | 46.0 | | |
| B3LYP/cc-pVTZ//B3LYP/cc-pVDZ | 41.5 | 38.1 | | |
| B3LYP/6-311+G(d,p)//B3LYP/cc-pVDZ | 40.1 | 35.9 | | |
| BLYP/6-311+G(d,p)//B3LYP/cc-pVDZ | 41.5 | 39.8 | | |
| BP86/6-311+G(d,p)//B3LYP/6-311+G(d,p) | 41.4 | 40.8 | | |
| B3LYP/6-311+G(d,p)//B3LYP/aug-cc-pVDZ | 39.6 | 38.9 | | |
| B3LYP/aug-cc-pVDZ//B3LYP/aug-cc-pVDZ | 38.8 | 38.1 | 44.0 | 37.2 |
| B3LYP/6-311+G(d,p)//B3LYP/6-311+G(d,p) | 39.8 | 39.0 | 41.7 | 35.8 |
| CCSD(T)/6-311+G(d,p)//B3LYP/6-311+G(d,p) | 34.9 | 36.4 | 33.3 | 35.1 |
| CCSD(T)/6-311+G(2d,2p)//B3LYP/6-311+G(d,p) | 34.6 | 35.9 | 33.8 | 34.8 |
| CCSD(T)/aug-cc-pVDZ//B3LYP/aug-cc-pVDZ | 36.5 | 37.3 | | |
| CCSD(T)6-311+G(d,p)//B3LYP/aug-cc-pVDZ | 34.8 | 36.3 | | |
| expt | 35 ± 3 | 39 ± 3 | | |

**TABLE 6: Energy Partition at RHF/Basis 1 for $Li^+$ and $Cu^+$ Complexes with One and Two Ligands[a]**

| complex | EX | ES | PL1 | PL2 | CT1 | CT2 | $\Delta E$ | complex | EX | ES | PL1 | PL2 | CT1 | CT2 | $\Delta E$ |
|---|---|---|---|---|---|---|---|---|---|---|---|---|---|---|---|
| $Cu^+-FH$ | 17.5 | −27.1 | −1.2 | −8.1 | −1.8 | −1.5 | −18.1 | $Li^+-FH$ | 6.0 | −23.3 | 0.0 | −9.1 | 0.0 | −2.3 | −24.7 |
| $Cu^+-OH_2$ | 39.2 | −54.8 | −2.9 | −18.2 | −3.4 | −2.2 | −32.0 | $Li^+-OH_2$ | 13.5 | −40.7 | 0.0 | −11.8 | 0.0 | −3.4 | −36.8 |
| $Cu^+-NH_3$ | 64.2 | −79.7 | −4.5 | −35.0 | −4.7 | −6.5 | −42.4 | $Li^+-NH_3$ | 19.2 | −48.9 | 0.0 | −15.4 | 0.0 | −4.6 | −41.3 |
| $Cu^+-ClH$ | 27.3 | −24.3 | −3.9 | −15.4 | −1.8 | −4.5 | −13.8 | $Li^+-ClH$ | 7.8 | −11.2 | 0.0 | −8.4 | 0.0 | −6.4 | −15.2 |
| $Cu^+-SH_2$ | 44.6 | −43.3 | −6.6 | −32.1 | −2.9 | −6.2 | −25.4 | $Li^+-SH_2$ | 10.8 | −19.4 | 0.0 | −13.2 | 0.0 | −7.6 | −23.0 |
| $Cu^+-PH_3$ | 59.5 | −61.1 | −9.0 | −28.1 | −4.2 | −13.6 | −35.3 | $Li^+-PH_3$ | 12.7 | −23.7 | 0.0 | −11.8 | 0.0 | −7.6 | −27.2 |

[a] All values are in kcal/mol.

**TABLE 7: Net Results from Morokuma Analysis at RHF/Basis 1 for $Li^+$ and $Cu^+$ Complexes**

| | $Cu^+$ | | | $Li^+$ | | | | | |
|---|---|---|---|---|---|---|---|---|---|
| ligand | EX + ES | PL | CT | EX + ES | PL | CT | $\Delta ES(Li^+-Cu^+)$ | $\Delta PL(Li^+-Cu^+)$ | $\Delta CT(Li^+-Cu^+)$ |
| FH | −9.6 | −9.2 | −3.3 | −17.3 | −9.1 | −2.3 | −7.7 | 0.1 | 1.1 |
| $OH_2$ | −15.6 | −21.6 | −5.6 | −27.2 | −11.8 | −3.4 | −11.6 | 9.8 | 2.2 |
| $NH_3$ | −15.5 | −44.0 | −11.2 | −29.7 | −15.5 | −4.6 | −14.2 | 28.5 | 6.6 |
| ClH | 3.0 | −19.8 | −6.3 | −3.4 | −8.4 | −6.4 | −6.4 | 11.4 | −0.1 |
| $SH_2$ | 1.3 | −44.0 | −9.2 | −8.2 | −13.2 | −7.6 | −9.5 | 30.8 | 1.6 |
| $PH_3$ | −1.6 | −43.1 | −17.9 | −11.0 | −11.8 | −7.6 | −9.4 | 31.3 | 10.3 |

more stabilizing for $NH_3$ by18.6 kcal/mol, and the exchange repulsion is 4.7 kcal/mol more destabilizing for $NH_3$. The net result is a more stabilizing effect for $NH_3$ by 8.6 kcal/mol, which coincides with the above-reported difference. Effects of other pairs of ligands (HF vs HCl and $H_2O$ vs $H_2S$) can be estimated from the Morokuma analysis, but in a qualitative manner as the binding energies of those pairs are sensitive to the level of theory. The effect of ligand polarization (PL2) is much higher than the polarization of $Cu^+$ (PL1). With the exception of FH and $H_2O$ ligands, CT1 (CT from M → ligand) is lower than CT2 (i.e., from L → M). All ligands but FH bind strongly with $Cu^+$ than with $Li^+$. This can be attributed to the higher exchange repulsion in the case of $Cu^+FH$, in addition to the hard−soft acid−base explanation. Electrostatic and polarization terms are primarily responsible for the interaction of different ligands with $Li^+$. If we look at $Li^+NH_3$ and $Li^+PH_3$, we find that ES is higher for the former (48.9 vs 23.7 kcal/mol) and PL is 3.7 kcal/mol in favor of $NH_3$.

## Conclusions

In this paper we have investigated the electronic structures and binding energies of $Li^+/Cu^+(XH)_n$ complexes, $n = 1,2$ and

X = F, Cl, OH, SH, $NH_2$, $PH_2$. We can summarize our results as follows:

The second ligand in $Cu^+$ complexes has higher binding energies compared to the first one because of increasing $sd_\sigma$ hybridization, polarization, charge transfer, and electrostatic interaction.

DFT methods reverse the order for the first two ligands but ab initio at post-HF levels give the correct order due to the improvement of the $sd_\sigma$ hybridization. B3LYP can probably describe the electrostatic interaction like $Li^+$ complexes but it overestimates the CT interaction involved in $Cu^+$ complexes and tends to overestimate the binding energy.

In general, geometry optimization using B3LYP with DZP or TZP gives good geometries. Diffuse functions are also important for proper description of the electron transfer and for producing accurate properties for the ligands, like geometry, dipole moment, etc. Final energy calculations at MP2 achieve the desired accuracy. Therefore, there is no need to go beyond MP2 for such closed-shell systems.

The geometry change occurring in $PH_3$ upon complexation was explained in term of $sp^3$ hybridization in the P atom as well as the electrostatic repulsion between positively charged hydrogen atoms.

**Acknowledgment.** We gratefully acknowledge financial support from the Ministry of Education, Science and Culture, Japan. A.M.E-N. is indebted to a fellowship from the Japan Society for the Promotion of Science (JSPS).

## References and Notes

(1) Magnera, T. F.; David, D. E.; Stulik, D.; Orth, R. G.; Jonkman, H. T.; Michl, J. *J. Am. Chem. Soc.* **1989**, *111*, 5036.

(2) Holland, P. M.; Castleman, Jr., A. W. *J. Chem. Phys*. **1982**, *76*, 4195.

(3) Walter, D.; Armentrout, P. B. *J. Am. Chem. Soc*. **1998**, *120*, 3176.

(4) Armentrout, P. B. *Acc. Chem. Res*. **1995**, *28*, 430.

(5) Dalleska, N. F.; Homma, K.; Sunderlin, L. S.; Armentrout, P. B. *J. Am. Chem. Soc*. **1994**, *116*, 3519.

(6) Clemmer, D. E.; Armentrout, P. B. *J. Phys. Chem.* **1991**, *95*, 3084.

(7) Magnera, T. F.; David, D. E.;. Michl, J. *J. Am. Chem. Soc*. **1989**, *111*, 4100.

(8) Marinelli, P. J.; Squires, R. R. *J. Am. Chem. Soc.* **1989**, *111*, 1401.

(9) Keesee, R. G.; Castleman, Jr., A. W. *J. Chem. Phys. Ref. Data* **1986**, *15*, 1011.

(10) Woodin, R. L.; Beauchamp, J. L. *J. Am. Chem. Soc.* **1978**, *100*, 501.

(11) Bene, J. E. D. *J. Phys. Chem*. **1996**, *100*, 6284.

(12) Feller, D.; Glendening, E. D.; Kendall, R. A.; Peterson, K. A. *J. Chem. Phys*. **1994**, *100*, 4981.

(13) Glendening, E. D.; Feller, D. *J. Phys. Chem*. **1995**, *99*, 3060.

(14) Glendening, E. D. *J. Am. Chem. Soc*. **1996**, *118*, 2473.

(15) Feller, D.; Glendening, E. D.; Woon, D. E.; Feyereisen, M. W. *J. Chem. Phys*. **1995**, *103*, 3526.

(16) Magnusson, E. *J. Comput. Chem*. **1994**, *16*, 1027.

(17) Periole, X.; Allouche, D.; Daudey, J.-P.; Sanejouand, Y.-H. *J. Phys. Chem. B* **1997**, *101*, 5018.

(18) Hoyau, S.; Ohanessian, G. *Chem. Phys. Lett*. **1997**, *280*, 266.

(19) Hoyau, S.; Ohanessian, G. *J. Am. Chem. Soc.* **1997**, *119*, 2016.

(20) Bowmaker, G. A.; Pabst, M.; Roesch, N.; Schmidbauer, H. *Inorg. Chem*. **1993**, *32*, 880.

(21) Re, N.; Rosi, M.; Sgamellotti, A.; Floriani, C.; Solari, E. *J. Mol. Struct. (THEOCHEM)* **1993**, *284*, 95.

(22) El-Nahas, A. M.; Tajima, N.; Hirao, K. *J. Mol. Struct. (THEOCHEM)* **1999**, *469*, 201.

(23) Luna, A.; Amekraz, B.; Tortajada, J. *Chem. Phys. Lett.* **1997**, *266*, 31.

(24) Bauschlicher, Jr., C. W.; Langhoff, S. R.; Partridge, H. *J. Chem. Phys*. **1991**, *94*, 2068.

(25) Bauschlicher, Jr., C. W.; Langhoff, S. R.; Partridge, H. *J. Chem. Phys.* **1991**, *95*, 5142.

(26) Langhoff, S. R.; Bauschlicher, Jr., C. W.; Partridge, H.; Sodupe, M. *J. Phys. Chem.* **1991**, *95*, 10677.

(27) Rosi, M.; Bauschlicher, Jr., C. W. *J. Chem. Phys*. **1989**, *92*, 1876.

(28) (a) Rosi, M.; Bauschlicher, Jr., C. W. *J. Chem. Phys*. **1989**, *90*, 7264. (b) Maitre, P.; Bauschlicher, Jr., C. W. *J. Phys. Chem.* **1993**, *97*, 11912.

(29) Schneider, W. F.; Hass, K. C.; Ramprasad, R.; Adams, J. B. *J. Phys. Chem.* **1996**, *100*, 6032.

(30) Hass, K. C.; Schneider, W. F. *J. Phys. Chem*. **1996**, *100*, 9292.

(31) Bauschlicher, Jr., C. W.; Ricca, A.; Partridge, H.; Langhoff, S. R. *Recent Advances in Density Functional Methods*; Chong, D. P., Ed.; World Scientific: Singapore, 1997; Chapter 6, p 196.

(32) Bauschlicher, Jr., C. W.; Langhoff, S. R.; Partridge, H. *Modern Electronic Structure Theory*; Yarkony, D. R., Ed.; World Scientific: Singapore, 1995; Chapter 21, p 1280.

(33) Pavlov, M.; Siegbahn, P. E. M.; Sandstrom, M. *J. Phys. Chem.* **1998**, *102*, 219.

(34) Trachtman, M.; Markham, G. D.; Glusker, J. P.; George, P.; Bock, C. W. *Inorg. Chem.* **1998**, *37*, 4421.

(35) Feller, D.; Glendening, E. D.; De Jong, W. A. *J. Chem. Chem.* **1999**, *110*, 1475.

(36) (a) Lee, C.; Yan, W.; Parr, R. G. *Phys. Rev.* **1988**, *B37*, 785. (b) Becke, A. D. *J. Chem. Phys.* **1993**, *98*, 5648.

(37) Frisch, M. J.; Frisch, A.; Foresman, J. M. *Gaussian 94 User's Reference*; Gaussian Inc.: Pittsburgh, PA 1998.

(38) Hay, P. J.; Wadt, W. R. *J. Chem. Phys*. **1985**, *82*, 299.

(39) Morokuma, K. *J. Chem. Phys*. **1971**, *55*, 1236.

(40) Schmidt, M. W.; Baldridge, K. K.; Boatz, J. A.; Elbert, S. T.; Gorden, M. S.; Jensen, J. H.; Koseki, S.; Matsunaga, N.; Nguyen, K. A.; Su, S.; Windus, T. L.; Depuis, M.; Montgomery, Jr., J. A. *J. Comput. Chem*. **1993**, *14*, 1347.

(41) Glendening, E. D.; Reed, A. E.; Carpenter, J. E.; Weinhold, F. *NBO 3.0*, Theoretical Chemistry Institute and Department of Chemistry, University of Wisconsin, Madison, WI 53706.

(42) Cotton, F. A.; Wilkinson, G. *Advanced Inorganic Chemistry*, 5th ed.; John Wiley & Sons: New York, 1988.

(43) Pearson, R. G. *J. Am. Chem. Soc*. **1963**, *85*, 3533.

(44) El-Nahas, A. M. Ph.D. Thesis, El-Menoufia university, Shebin El-Kom, Egypt, 1993.

(45) Kapp, J.; Schade, C.; El-Nahas, A. M.; Schleyer, P. v. R. *Angew. Chem., Int. Ed. Engl.* **1996**, *35*, 2236.